Inverse Blech Length Phenomenon in Thin-Film Stripes

Nalla Somaiah and Praveen Kumar[*]

Department of Materials Engineering, Indian Institute of Science, Bangalore 560012

For decades, thin-film interconnects have been designed considering that the electric-current-induced mass transport or electromigration in thin films decreases with the reduction in the length of the film. This phenomenon is often called the Blech length effect, which dictates the seizure of electromigration if the product of the current density and the film length is smaller than a critical value. We report a phenomenon in Cu film stripes fabricated as per Blech configuration, where we observe that the electric-current-driven mass transport at the cathode increases as the sample length is reduced. We call this phenomenon the "inverse Blech length effect." Furthermore, the mass transport at the cathode in Cu film increases linearly with the inverse of the sample length. Finite-element analysis reveals an increase in the self-induced temperature gradients, which are very large to induce thermomigration in Cu, at the ends of Cu film with a decrease in the sample length. Therefore, the contribution of thermomigration increases in the overall mass transport at the cathode as the sample length is decreased. The ensuing electromigration-thermomigration coupling is used to qualitatively explain the observation of the inverse Blech length phenomenon. The findings in this work open avenues for the design of device-level interconnects in microelectronic devices.

I. INTRODUCTION

Electromigration, which transports matter directionally from one of the electrodes to another upon passage of electric current, is a major reliability issue associated with thin-film interconnects in integrated circuits (ICs) [1]. Electromigration often becomes important at very high current densities (e.g., $> 10^8$ A/m^2) and it results in mass depletion at the cathode and mass accumulation at the anode in most of the solid metals, such as Cu, Al, Au, etc. Because of the mass depletion and the mass accumulation at the cathode and the anode, respectively, open circuit and short circuit, respectively, occur at these two ends of the Cu (as well as Al) film. One of the methods for avoiding electromigration in thin film interconnects is fabricating shorter interconnects [2]. This method is based on the Blech length effect, named after Ian A. Blech, who proposed that the extent of the electromigration in a conductor would decrease with a decrease in the sample size so that it will completely seize when the product of the current density j and the sample length l is smaller than a critical value [2,3]. For an application where the current density cannot be arbitrarily affixed to a lower value, the above guideline translates into designing interconnects with a length smaller than a critical length l_c, which is often called the Blech length [see Fig. 1(a)] [2,3].

The Blech length effect is an outcome of the existence of a stress gradient, which is generated in response to the gradient of vacancies, created due to electromigration, from the anode to the cathode [2]. Accordingly, the anode is at a higher compressive stress, due to the depletion of the vacancies below the equilibrium concentration, as compared to the cathode. Therefore, the generated stress gradient acts in the direction opposite to the atomic transport due to the electromigration. Accordingly, as schematically shown in Fig. 1(b), the mass transports due to the electromigration and the self-generated stress gradient are in the opposite directions, with a finite probability that the latter can inhibit the mass transport due to the electromigration. In the interconnects of the length equal to the Blech length (i.e., l_c), the force on atoms due to the stress gradient in the interconnect exactly matches the force due to the electric field, and hence, these interconnects do not show any mass transport. This phenomenon suggests that electromigration will not occur in interconnects with length smaller than l_c. However, it should be noted that the generation of the stress gradient is dependent on the electromigration and, hence, the stress gradient (and, accordingly, mass transport) will not exist in the absence of electromigration [3]. Interestingly, there are reports suggesting a need for finite electromigration before the stress gradient can be established and, hence, it is not possible to strictly avoid electromigration altogether [4]. However, electromigration can be greatly minimized due to the Blech length effect.

Mathematically, the equilibrium between stress gradient and electromigration forces, which is responsible for the
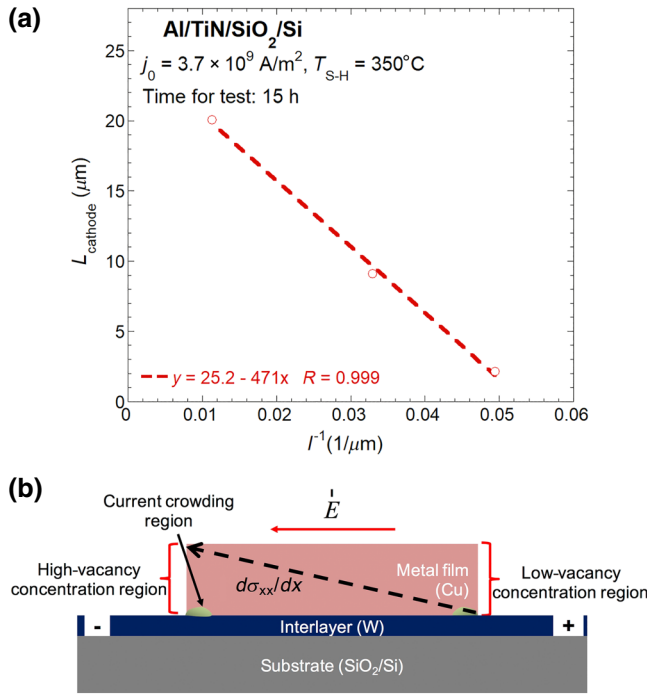
———————
[*]praveenk@iisc.ac.in

FIG. 1.   (a) Variation of the length of the depletion zone at the cathode in an unpassivated Al sample as a function of the inverse of the sample length l. The data are reproduced from Fig. 1 of Ref. [3] after obtaining permission from Elsevier. The broken line is the best linear curve fit, whose equation is given in the legend. (b) Schematic illustration of the origin of the stress gradient and its action. Excess concentration of vacancies accumulates near the cathode, while the anode is relatively depleted of vacancies, thereby resulting in the stress gradient (shown using a broken arrow) in the thin film. For relevance, the sample is shown in the Blech configuration, wherein a short stripe of metal film is deposited on a substrate with a long interlayer in between.

Blech length effect, can be expressed as follows [3,5,6]:

$$F_d = Z^* eE - \Omega \frac{\partial \sigma_{xx}}{\partial x} = 0, \qquad (1)$$

where F_d is the net forward force on an atom from the cathode to the anode; Z^*, e, and E are the effective charge number, charge of an electron, and the electric field, respectively; Ω is atomic volume; σ_{xx} is the normal stress along the length of the sample and x is the coordinate along the sample length (so that $d\sigma_{xx}/dx$ is the stress gradient). In Eq. (1), the sign of Z^* is selected so that electromigration force acts toward the anode, whereas the sign of $d\sigma_{xx}/dx$ is chosen so that it acts toward the cathode. Equation (1) predicts a decrease in the forward force on the atom as the stress gradient increases; this prediction explains the behavior shown in Fig. 1(a). Now, replacing E with $j\rho$, where ρ is the electrical resistivity, for metallic conductors in Eq. (1) and assuming uniform stress gradient (so that $d\sigma_{xx}/dx = \Delta\sigma_{xx}/l$), one obtains the following relationship for the product of the current density and length of

the sample for the condition of seizure of electromigration (i.e., $F_d = 0$):

$$(jl)_c = \frac{\Omega \Delta \sigma_{xx}}{eZ^* \rho}. \qquad (2)$$

The product jl in Eq. (2) is often called the critical product (and, hence, the use of the subscript c). Since the critical product of j and l is determined by the threshold stress (i.e., $\Delta\sigma_{xx}$) that can be supported by interconnects, $\Delta\sigma_{xx}$ can be taken as the yield strength in the compression of the material assuming ideal plastic behavior [3]. In general, $\Delta\sigma_{xx}$ is understood to scale with the yield stress of the metallic film.

It should be noted that the critical product also depends on several other parameters that are not mentioned explicitly in Eq. (2), such as the material microstructure, choice of diffusion barrier layer [7], capping layers, anodic oxide thickness [8,9], configuration of interconnects [10], etc. Furthermore, it was recently shown that surface instability under large thermal stress conditions can drive mass transport in interconnects even below the Blech length [11]. Hence, there is a need for critical evaluation of Eq. (2). In this context, it is also important to evaluate the existence of the Blech length effect in the presence of thermomigration due to the self-induced temperature gradient. This is especially so as thermomigration is becoming important in the modern interconnects due to spontaneous establishment of the self-induced temperature gradients of very high magnitudes ($>10^5$ K/m) [12]; this can be generated due to the passage of currents of high densities through interconnects having joints, junctions, and bends (which are present as an outcome of multilevel architecture).

Interestingly, the effect of localized current crowding and, hence, temperature gradients on the Blech length effect has not been studied systematically, as all previous studies have used only uniform current density. As a matter of fact, Abbasinasab and Sandowska [10] and Straub et al. [13] suggested that the thermomigration would not affect the mass transport during the electromigration in interconnects. However, as shown in our previous works [14,15], the above is not true, especially if a large temperature gradient is generated due to current crowding at the ends of the Cu film. Interestingly, the mass transport at the cathode is enhanced and "anomalous" backward mass transport occurs at the anode (forming a depletion zone at the anode also) due to the (linear) coupling between the electromigration and thermomigration [14,15]. Accordingly, the main objectives of this work are to reevaluate the effects of the length of conducting film (Cu), prepared as per the Blech structure [see Fig. 1(b)], on the temperature gradients, regular forward mass transport at the cathode, and, eventually, the existence of the Blech length effect. We show that the mass transport and, hence, the extent of the depletion zone at the cathode increase with a decrease in the sample length; we call this phenomenon the inverse
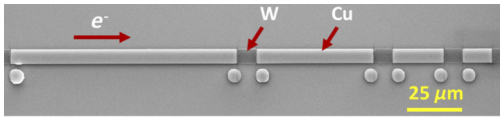
FIG. 2. A low-magnification SEM micrograph of a sample comprising multiple stripes of Cu film deposited on a SiO_2/Si substrate with a long, continuous 30-nm-thick W interlayer. The segmented Cu film has lengths of 100, 52, 22, and 12 μm from left to right. Small circular pads, which do not carry any current, near the ends of each Cu stripe are deposited to mark the initial boundaries of the Cu stripe.

Blech length effect. This study is particularly important in the context of modern multilevel ICs, wherein there are numerous bends, joints, and junctions [16,17]; these geometric features automatically induce current crowding and, hence, localized high temperature as well as self-induced temperature gradients.

II. EXPERIMENTAL PROCEDURE

A. Sample fabrication

Samples with Cu as the test thin metal film, W as the interlayer, and SiO_2/Si as the substrate are fabricated as per the Blech configuration [see Fig. 1(b)] [3,18]. The details of sample fabrication are given in Ref. [14] and they are briefly described here for continuity. A 100-nm-thick layer of SiO_2 is grown on a Si substrate using dry oxidation. Subsequently, a continuous and long stripe of 30-nm-thick W film is deposited using direct current (dc) magnetron sputtering. Finally, segmented Cu films of 150-nm thickness, with each segment having different lengths, are deposited on the W interlayer using dc magnetron sputtering. Lengths of the Cu segments are 100, 52, 22, and 12 μm in this sequence from the cathode to the anode. Figure 2 shows a low-magnification micrograph, obtained using a scanning electron microscope (SEM), of a representative sample. The width of both W and Cu films is 7 μm. Segmented samples of Al thin film of similar lengths (e.g., 10, 20, 50, and 100 μm) were fabricated by Blech in the original study on Blech length phenomenon [2]. Hence, in this first report, we fabricate samples of Cu films of similar dimensions for a direct comparison.

B. Testing procedure

The fabricated samples are tested by passing an electric current in a vacuum chamber operating at a base pressure of $\leq 5 \times 10^{-6}$ mbar. An electric current of nominal density j_0, calculated by dividing the total current by the combined cross-sectional area of W and Cu films, of approximately 4×10^{10} A/m^2 is passed through the sample. The temperature of the substrate $T_{S\text{-}H}$, is maintained at 250°C using an external substrate heater throughout the test. An electromigration test is conducted up to a certain time, such as 30,

100, and 180 min. Upon conclusion of the tests, the sample is observed using SEM and the extent of the depletion zone at the cathode is measured.

C. Finite-element analysis

Finite-element analysis (FEA) is performed using COMSOL Multiphysics® software to observe the effects of the length of the Cu stripes (see Fig. 2) on the current crowding and distribution of the temperature field (including the temperature gradient) in the sample, especially at the ends of the Cu stripes. The obtained temperature field is then used to ascertain the role of thermomigration in the forward mass transport at the cathode. The geometrical model of the sample has the same dimensions as those of the samples used in the experiments. In addition, thickness-dependent electric resistivity values of W and Cu films are used, as follows: $\rho_W = 7.7 \times 10^{-8}$ Ωm for 30-nm-thick W film [19] and $\rho_{Cu} = 2.2 \times 10^{-8}$ Ωm for 150-nm-thick Cu film. The electrical resistivity of SiO_2 and Si is assumed to be infinity, so that the entire current passed through only two metal films. Heat loss due to radiation only is assumed in FEA, as the tests are performed in a vacuum chamber.

III. RESULTS AND DISCUSION

Figure 3 shows a set of representative results obtained from tests performed for 100 min by passing electric current of a nominal current density of approximately 4×10^{10} A/m^2 through the sample, while maintaining the substrate heater temperature of 250°C. As shown in Fig. 3(a), only the forward migration at the cathode is observed at this magnification (i.e., mass transport in the backward direction at the anode cannot be discerned). In addition, numerous hillocks form near the anode. Hence, the mass transport observed in these tests resembles that of a *classic* electromigration test performed using Blech structure. However, Fig. 3(b) shows that the extent of the forward migration monotonically increases with the decrease in the length of Cu stripes. Based on the curve-fitting analysis shown in Fig. 3(b), it can be inferred that the extent of the depletion zone (or forward migration at the cathode) L_{cathode} increases linearly with the inverse of the stripe (or sample) length l^{-1}. Therefore, a comparison of Figs. 3(b) and 1(a), which shows the *classic* Blech length effect, reveals observation of the inverse Blech length phenomenon in these samples under the employed experimental conditions. Although, as mentioned earlier, some deviations from the classic Blech length effect have been reported in the past [11], our study reports the inverse Blech length phenomenon in Cu films due to *only* electric current loading.

It should be noted that if these tests are performed for very long period (e.g., up to the time when the resistance of the entire sample increased by 20%), a noticeable mass transport at the anode (i.e., "anomalous" backward mass
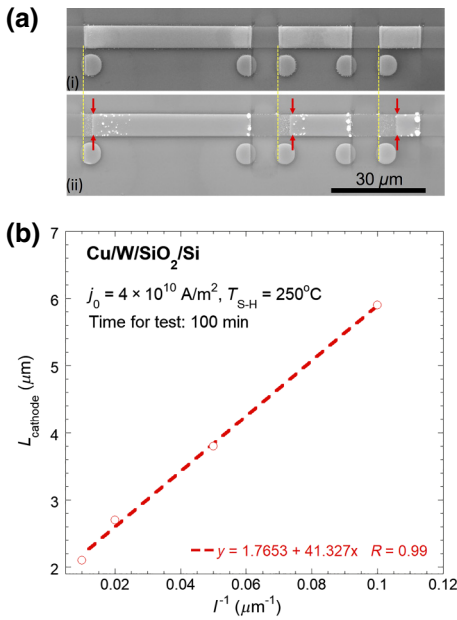
(a)

(b)

FIG. 3. (a) A set of low-magnification SEM micrographs showing several Cu stripes (i) before and (ii) after 100 min of electric current loading. Broken vertical lines indicate the initial position of the Cu stripe, whereas the pair of solid vertical arrows indicates the edges of the Cu film after the test. (b) Variation of the extent of the forward mass transport at the cathode L_{cathode} as a function of the inverse of the stripe length l^{-1}. The broken line shows the best linear curve fitted through the data points and the legend at the bottom right of the graph shows the corresponding best-fit equation, along with the value of the curve-fitting parameter R.

(a)

(b)

FIG. 4. Variation of the extent of the forward migration (or depletion zone) at the cathode L_{cathode} as a function of (a) the inverse of the sample or stripe length (l^{-1}) and (b) the time over which a test was run (t_{test}). The symbols represent the test data, whereas the curves passing through the data points are the best fit linear curves.

transport) is also observed [14,15]. We deliberately avoid performing tests for such long durations here so that we can observe only the forward mass transport at the cathode, as often reported in the classic electromigration tests using Blech-type samples. This procedure allows direct comparison between the phenomenon observed in this study and the classic Blech length effect.

Since the test duration can affect the extent of the depletion zone at the anode, and, perhaps, also the dependence of the forward mass transport on the stripe length, tests using the same nominal current density of approximately 4×10^{10} A/m^2 and the substrate heater temperature of 250°C are performed for 30 and 180 min also. The obtained results are shown in Fig. 4. As shown in Fig. 4(a), irrespective of the test duration, the extent of the forward migration monotonically increases with the inverse of the sample length. A careful observation of Fig. 4(a) reveals that the slope of the best-fit linear curves increases (rather linearly; see Fig. S1 in Ref. [20]) with the test duration, thereby suggesting that the severity of the dependence on the sample length increases significantly with the time of the tests. This characteristic of the inverse Blech length
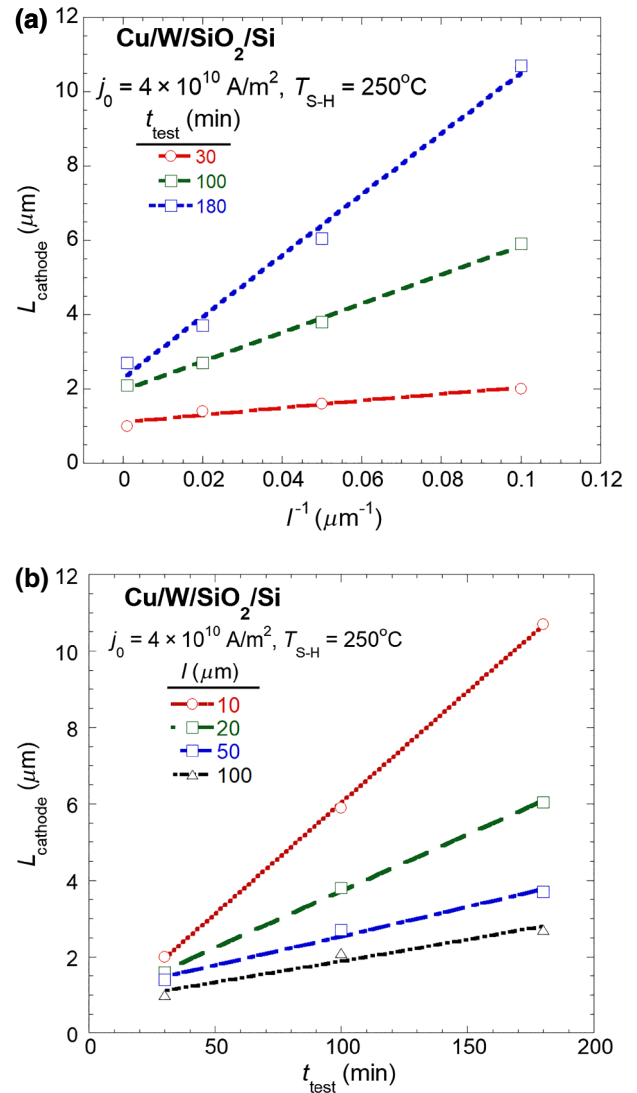
phenomenon is also in direct contrast with the Blech length effect, which is considered to be invariant with time.

The data shown in Fig. 4(a) are replotted in Fig. 4(b) to reveal the effect of the test duration on the forward mass transport at the cathode for various stripe lengths. Within the limitation of the number of experimental data points, it appears that the forward mass transport at the cathode increases linearly with the test duration for all samples (i.e., irrespective of sample length). A linear increase in the extent of the mass transport with time suggests a constant drift velocity, which is a signature of stable test conditions (wherein any nonlinearity due to local damages is not noticeable). Figure 4(b) also reveals that the kinetics of

mass transport is the fastest in the smallest of the samples (i.e., the 10-μm-long Cu stripe in this study) and it slows down with an increase in the sample length. This result suggests that additional driving forces, which increase with a decrease in the sample length, must be acting on these samples in addition to the anticipated electromigration force and the self-induced stress gradient. These additional forces may be responsible for the inverse Blech length phenomenon and, hence, FEA simulations are performed to investigate the origin of such forces, as described next.

IV. FINITE-ELEMENT ANALYSIS

As can be inferred from Fig. 1(b), the entire electric current passes through the W interlayer in between the Cu stripes and it is distributed in between the Cu film and W interlayer wherever the Cu stripes are deposited. Since 150-nm-thick Cu is relatively less resistive as compared to 30-nm-thick W, most of the current leaves the W interlayer to pass through the Cu film at its anode end and vice versa at its cathode end. Such a transition in the current path leads to significant current crowding at the Cu film ends, as schematically shown in Fig. 1(b). At these locations, the local current density and hence the temperature field (due to enhanced Joule heating) are relatively more intense (i.e., higher). Creation of such localized hot spots may also induce large temperature gradients between the edge and the center of the Cu film. Interestingly, FEA performed in Ref. [14] for such a sample geometry clearly showed that the temperature gradient generated at the ends of a 200-μm-long isolated Cu film can be as high as 10^5–10^6 K/m, which is significant enough to induce thermomigration [14]. It should be noted that thermomigration in Cu causes directional mass transport from a hot region to a cold region via a diffusion mechanism [12]. Since both thermomigration and electromigration are diffusion-based directional mass transport phenomena, they can couple with each other to alter the net mass transport in Cu film [14]. In particular, they act in the same direction at the cathode, i.e., from the hot cathode to the cooler center (which is at a higher electric potential), and, hence, augment each other. Since the thermomigration force, which acts in addition to the electromigration and the stress gradient acting on atoms in these samples, is directly proportional to the temperature gradient [21], the effect of the length of the sample, fabricated as per the Blech configuration, on the electric current density, temperature, and temperature gradient at the cathode end of each Cu stripe is determined using FEA.

Figure 5 shows the current density distribution (color coded) and line profiles of current density along the length of the stripe as well as along the width of the stripe at the center of each stripe. As shown in Figs. 5(a) and 5(b), the current density, irrespective of the sample length, is uniform over the entire Cu film except near the ends of the
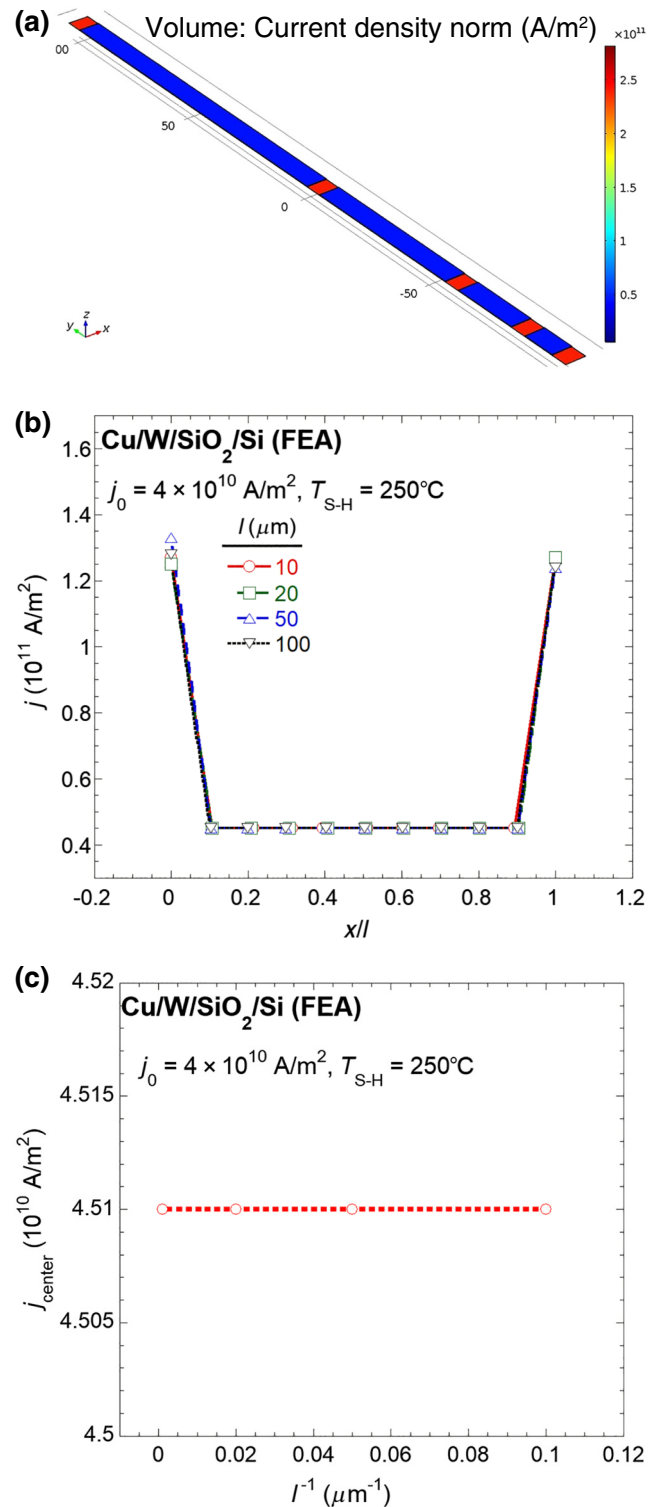

FIG. 5. (a) Distribution of the magnitude of the current density on the top surface of the sample. (b) Line profile showing the variation of the current density along the length of the sample. The x axis is normalized by dividing it by the total length of the stripe. See Fig. S2 in Ref. [20] for an enlarged view of the central region. (c) Variation of the current density in the central region (where it shows a saturation or minimum value) as a function of the inverse of the sample length.

Cu stripes. The average value of the current density at the ends is approximately 1.2×10^{11} A/m^2, which drops to the expected current density of approximately 4.5×10^{10} A/m^2 a little away from the ends [see Figs. 5(b) and 5(c)]. Therefore, the FEA simulations show the negligible effect of the stripe length on the current density near the edges as well as the center of the Cu film and, hence, the electromigration force on Cu atoms at the cathode and the overall film remains the same in all Cu stripes.

Figure 6 shows the temperature distribution in Cu stripes in the form of a color-coded map and line profile along the center of the stripe. As shown in Fig. 6(b) and consistent with Fig. 5, the temperature of the samples is relatively higher at the ends of the Cu stripes. Interestingly, Figs. 6(b) and 6(c) also reveal that the minimum temperature (i.e., in the central region of the sample) of the shorter samples is relatively greater than that of the longer samples. A best-fit curve analysis of the temperature profile shows a linear dependence of the minimum temperature on the inverse of the stripe length (i.e., $T \propto l^{-1}$) [see Fig. 6(c)].

Figure 7 shows the distribution of the temperature gradient, along with the line profiles of the same, for stripes with different lengths. As expected, the temperature gradients observed in these samples are very high, especially near the ends of the Cu stripes. Careful observation of Figs. 7(b) and 7(c) reveals that not only the temperature gradients at the edges of the films increase with a decrease in the stripe length, but also that the values of the temperature gradients in the middle sections, wherein they are the smallest, increase rapidly with a decrease in the sample length. A best-fit curve analysis of the temperature gradient at the center of the film shows a quadratic dependence of the minimum temperature gradient on the inverse of the stripe length (i.e., $T \propto l^{-2}$).

It should be noted that the average values of current density, temperature, and temperature gradients, as shown in Figs. 5–7, are extracted from the region just above the Cu-W interface, i.e., within the distance of 0.1 nm above the interface of Cu-W. In conclusion, FEA simulations show that the minimum temperature and the minimum temperature gradient (i.e., the corresponding values in the center of the Cu stripes), as well as the maximum temperature and the maximum temperature gradient (i.e., the corresponding values at the edge of Cu film), monotonically increase with a decrease in the stripe length. The effect of sample length on the current density is not significant. Using this set of observations, it can be stated that the driving forces for the thermomigration and electromigration relatively increase and remain constant, respectively, at the cathode, whereas the driving force for the stress-gradient-driven mass transport, which scales with the yield strength of the film, may, depending on the effect of temperature on the yield strength, decrease or remain constant with a decrease in the sample length. We develop a simple model based on the FEA results, which can be used to
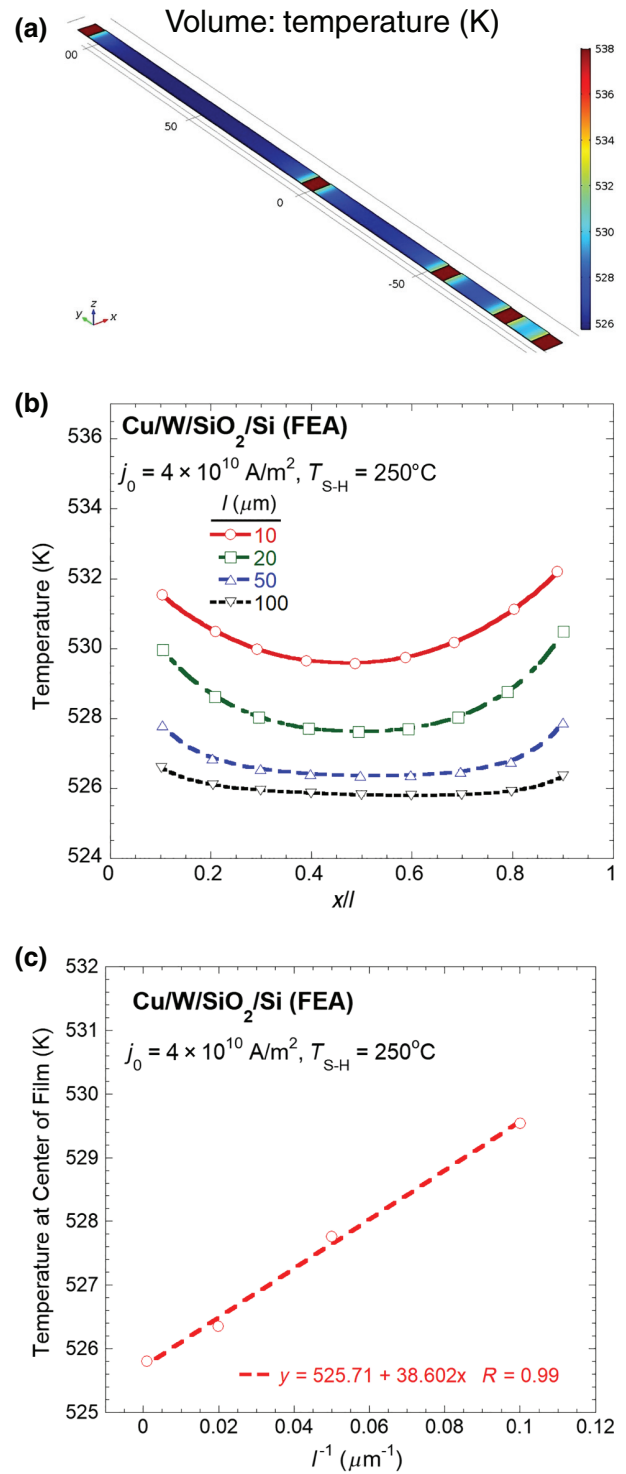

FIG. 6. (a) Distribution of temperature on the top surface of the sample. (b) Line profile showing the variation of temperature along the length of the sample. The x axis is normalized by dividing it by the total length of the stripe. See Fig. S3 in Ref. [20] for the variation of temperature up to the Cu film edges. (c) Variation of temperature in the central region (where it shows a saturated minimum value) as a function of the inverse of the sample length. The broken line is the best-fit curve fit, whose equation is given in the legend.
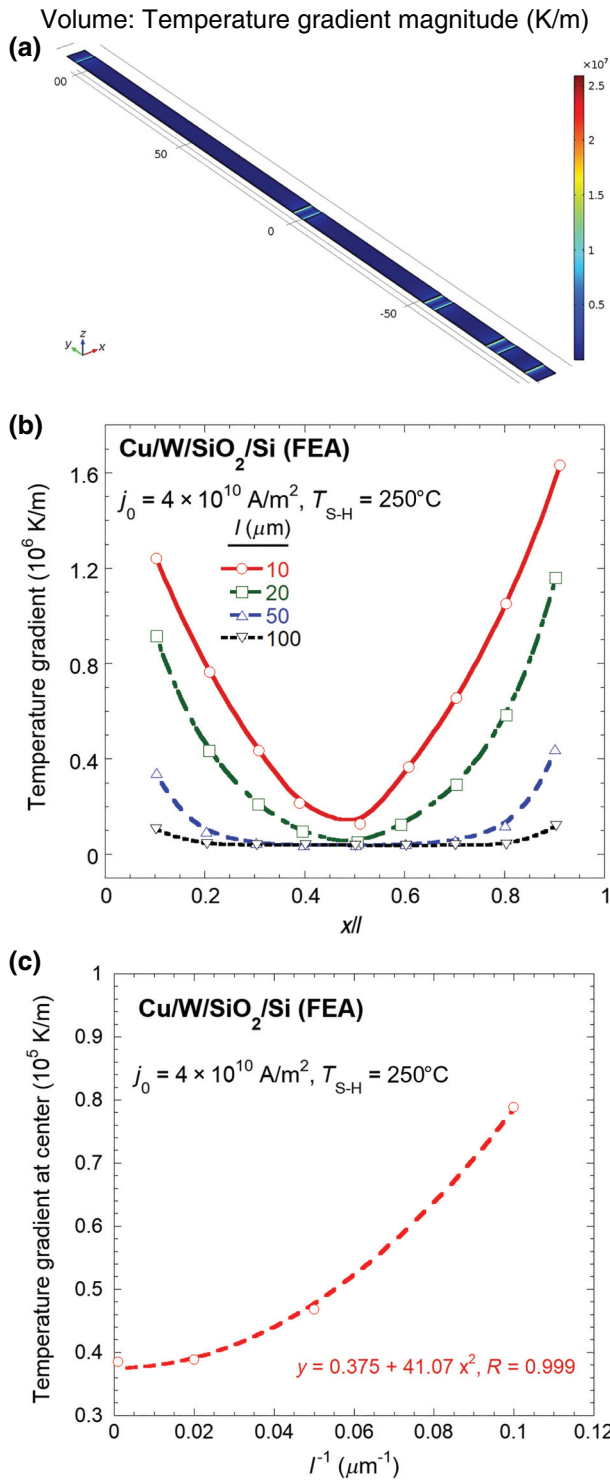
FIG. 7. (a) Distribution of the temperature gradient on the top surface of the sample. (b) Line profile showing the variation of the temperature gradient along the length of the sample. The x axis is normalized by dividing it by the total length of the stripe. See Fig. S4 in Ref. [20] for a variation of the temperature gradient up to the Cu film edges. (c) Variation of temperature gradient in the central region as a function of the inverse of the sample length. The broken line is the best-fit curve fit, whose equation is given in the legend.

explain the experimental observation of the inverse Blech length phenomenon.

To evaluate the condition for the seizure of the forward mass transport at the cathode, the forward-driving force due to the thermomigration (F_{tm}) and electromigration (F_{em}) must become equal to the backward-driving force due to the stress gradient (F_{sm}). In this limiting condition, one can write the following scalar equation:

$$
\begin{aligned}
F_d &= |F_{em}| + |F_{tm}| - |F_{sm}| \\
&= |Z^*eE| + \left|\frac{Q^*}{T}\frac{dT}{dx}\right| - \left|\Omega\frac{d\sigma_{xx}}{dx}\right| \\
&\approx |Z^*eE| + \left|3k\frac{dT}{dx}\right| - \left|\Omega\frac{d\sigma_{xx}}{dx}\right| = 0,
\end{aligned}
\tag{3}
$$

where Q^* and k are the heat of transport and the Boltzmann constant, respectively. Note that the value of Q^* is assumed to be equal to $3kT$ in Eq. (3), which is a reasonable assumption for solid metals [22]. Now, based on the FEA simulations [see Figs. 6(c) and 7(c)], the following expressions for effect of stripe length on the temperature and the temperature gradient can be assumed:

$$
T \sim A + \frac{B}{l},
\tag{4a}
$$

$$
\frac{dT}{dx} \sim C + \frac{D}{l^2},
\tag{4b}
$$

where A, B, C, and D are positive constants. Now, if the yield strength of the material σ_y is assumed to decrease linearly with the temperature, i.e., $\sigma_y = \sigma_{y,0} - k_1 T$, where $\sigma_{y,0}$ and k_1 are positive constants, the following can be used to estimate the stress gradient in a sample:

$$
\begin{aligned}
\frac{\Delta\sigma_{xx}}{l} &\sim \frac{\sigma_{y,o} - k_1(A + (B/l))}{l} = \frac{\sigma_{y,0} - k_1 A}{l} \\
&- \frac{k_1 B}{l^2} = \frac{F}{l} - \frac{G}{l^2},
\end{aligned}
\tag{5}
$$

where F and G are positive constants, such that $G < Fl$. Interestingly, Eq. (5) predicts that the stress gradient, which pushes atoms back toward the cathode and, hence, is responsible for the Blech length effect, will decrease with a decrease in the sample length. On the other hand, Eq. (4b) suggests an increase in the temperature gradient and, hence, an increase in the forward-migrating thermomigration force, with a decrease in the sample length. Hence, a comparison of Eqs. (4b) and (5) hint toward the "impossibility" of observing the Blech length phenomenon in the presence of significant electromigration-thermomigration coupling.
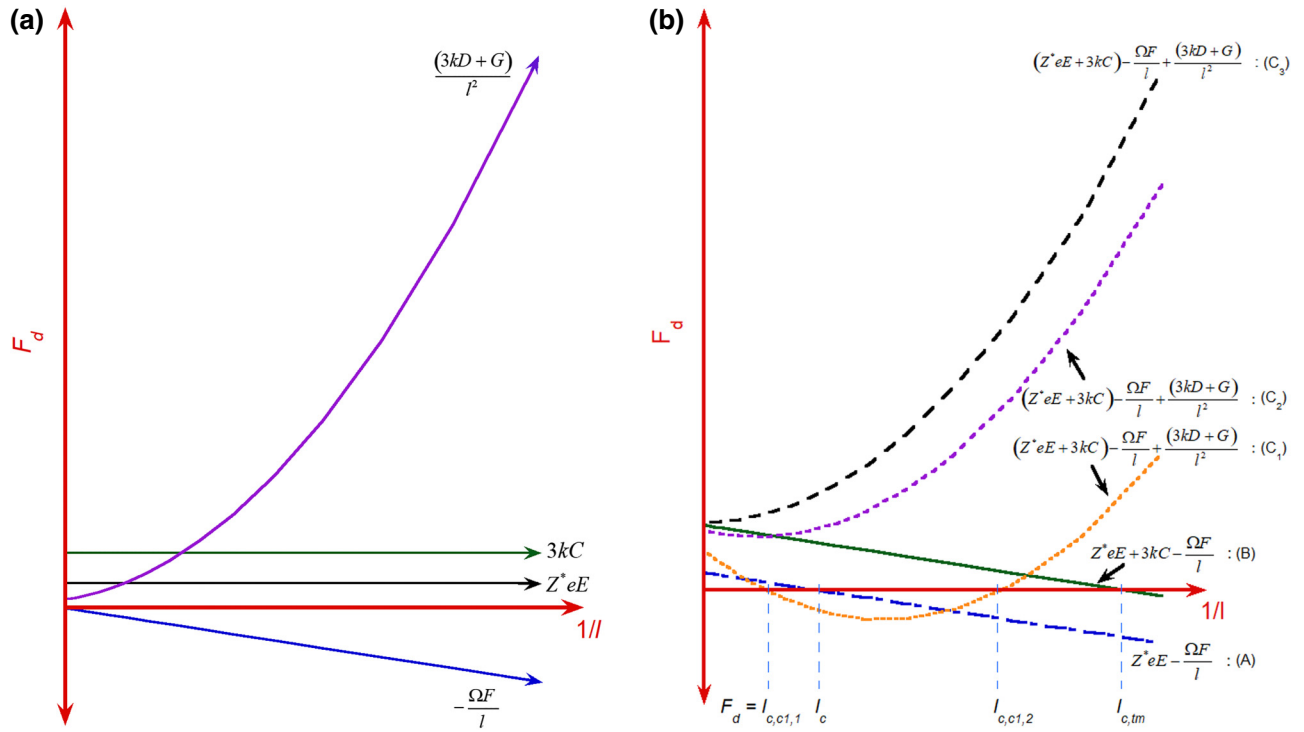
FIG. 8. Schematic illustration of (a) different terms on the right-hand side of Eq. (6) and (b) summation of them. The text such as (A), (B), (C_1), etc., at the end of the summation of terms represents a possibility. For example, possibility (A) represents the summation of Z^*eE (i.e., electromigration) and $\Omega F/l$ (i.e., stress gradient) terms. The curve showing the variation of $(3kD + G)/l^2$ in (a) corresponds to possibility (C_1) in (b).

Now, putting Eqs. (4b) and (5) into Eq. (3), one gets the following expression for the net forward-driving force F_d:

$$F_d = Z^*eE + 3k\left(C + \frac{D}{l^2}\right) - \Omega\left(\frac{F}{l} - \frac{G}{l^2}\right)$$

$$= (Z^*eE + 3kC) - \frac{\Omega F}{l} + \frac{3kD + G}{l^2}. \quad (6)$$

It should be noted that FEA results do not show that the sample length has any effect on the current density distribution in the sample and, hence, the electromigration term in Eq. (6) is assumed to be independent of sample length l. Equation (6) can be rewritten as follows:

$$F_d l^2 = (Z^*eE + 3kC)l^2 - \Omega F l + (3kD + G). \quad (7)$$

For the length at which the forward mass transport will stop or the Blech length effect will be observed, F_d will be 0, which implies finding a root of the quadratic equation given in the right-hand side of Eq. (7). Interestingly, the roots of the above quadratic equation can be real only if

$$\Omega^2 F^2 - 4(Z^*eE + 3kC)(3kD + G) > 0, \quad (8)$$

which may not always be possible. The sanity of Eq. (8) can be checked if the value of constants B and D in Eq. (4)

are taken to be zero for the condition when the sample length has no effect on the temperature field. If so, then the value of G, as given in Eq. (5), is also zero; thereby Eq. (8) simply implies that the existence of a positive compressive yield strength of a material (i.e., $F > 0$), which is always true, is needed for $F_d = 0$, i.e., satisfying the Blech length criteria. Hence, the deviation from the Blech length effect, as suggested by the full Eq. (8), is simply because of the dependence of the temperature and temperature gradient in the film on the sample length.

Various terms on the right-hand side of Eq. (6) are schematically shown in Fig. 8, wherein each term of Eq. (6) is shown by the solid arrows in Fig. 8(a) and their various sums are shown by the different curves in Fig. 8(b). As shown in Fig. 8(b), we can understand various outcomes of the superposition of electromigration, thermomigration, and stress-gradient-induced mass transports in terms of the following three broad possibilities:

(1) Possibility (A): Possibility (A) in Fig. 8(b) considers neither thermomigration (i.e., $C = D = 0$) nor the effect of length on the current crowding or temperature of the sample (i.e., $G = 0$) and, hence, it graphically depicts Eq. (1). Therefore, it is the same as the consideration made by Blech while deriving the idea of the Blech length effect [2,3]. As expected, this possibility gives a unique solution

for F_d to be zero at a length of l_c and implies the seizure of forward mass transport at the cathode if the length of the sample decreases below a critical length.

(2) Possibility (B): In addition to the electromigration and stress gradient, possibility (B) in Fig. 8(b) also includes the effect of thermomigration. However, it does not consider the effect of sample length on temperature and temperature gradient (i.e., $D = G = 0$). Like possibility (A), possibility (B) also shows that F_d will become zero at a length of $l_{c,\text{tm}}$ and there is no forward mass transport at the cathode in the samples with length smaller than $l_{c,\text{tm}}$. Hence, this possibility also shows a Blech-length-type phenomenon; however, the critical sample length is smaller than that observed during pure electromigration [or classic Blech length phenomenon, i.e., possibility (A)].

(3) Possibility (C): As observed in this study, the sample length affects the current crowding as well as the temperature gradient at the cathode and, hence, this possibility considers all of the terms in Eq. (6). However, depending on the value of $3kD + G$ relative to ΩF, one may expect one of the following three possibilities:

(i) Possibility (C_1): If the value of $3kD + G$ is very small as compared to ΩF, then one may expect a decrease in the forward migration at the cathode with a decrease in the sample length. Eventually, it leads to a condition wherein F_d is zero, e.g., at $l_{c1,1}$ and $l_{c1,2}$ in Fig. 8(b). In this scenario, one may expect zero forward migration for the samples of lengths in between $l_{c1,1}$ and $l_{c1,2}$, as $F_d < 0$. Under this condition, the samples with length greater than $l_{c1,1}$ show a monotonous decrease in the forward migration at the cathode with the decrease in the sample length, which is similar to the Blech length effect (with a possible nonlinear variation with $1/l$). However, forward migration at the cathode increases in the samples with length smaller than $l_{c1,2}$, which is akin to the inverse Blech length phenomenon. This result is most likely not the case in this study, as stripes of length as large as 100 μm show an inverse Blech length.

(ii) Possibility (C_2): If the value of $3kD + G$ is only moderately smaller than ΩF, then there is a transition from a decrease in the forward migration with a decrease in the sample length to an increase in the finite forward migration with a further decrease in the sample length. However, there is always a forward migration at the cathode, i.e., the mass transport never ceases. This study, which uses only four sample lengths, does not show a transition to a minimum forward mass transport, as predicted for this possibility. To ascertain if this is the dominant possibility in this sample (i.e., the Cu/W/Si system), tests on samples having longer lengths are warranted.

(iii) Possibility (C_3): If the value of $3kD + G$ is fairly large compared to ΩF, then the forward migration at the cathode monotonically increases with a decrease in sample length; however, such an increase slows down as the sample becomes very large. In this condition, it is possible for the increase in the forward mass transport at the cathode to appear linear in a small length interval, especially if the samples are long. This appears to be the case observed in this study; however, samples of longer lengths should be tested to predict the nonlinear, saturating behavior as shown in Fig. 8(b) [i.e., possibility (C_3)].

Irrespective of the above three conditions under the broad possibility (C), it can be stated that the net forward migration at the cathode always increases for very short samples, which is contrary to the classic Blech length effect and consistent with the observation of inverse Blech length phenomenon, as experimentally observed in this study. At the same time, it is also recommended to perform tests on longer as well as shorter samples, as compared to those tested in this study, to ascertain the dominant possibility [as predicted by Eq. (6)] as well as to show if the effect of thermomigration-electromigration saturates when the sample becomes very large.

In summary, upon decreasing the length of the sample, the following events take place in the presence of current crowding: (i) the back stress, which opposes the forward mass transport at the cathode, decreases due to the rise in the temperature and, hence, the corresponding decrease in the yield strength of the material; (ii) the forward-migrating thermomigration increases due to the increase in the self-induced temperature gradient (as well as temperature); and (iii) the electromigration driving force remains constant (or slightly increases due to the increase in temperature). As a result of these three events, the net driving force for the forward mass transport does not decrease (but rather increases) with a decrease in the sample length and, hence, the classical Blech length effect is not observed in the presence of thermomigration-electromigration-coupling-induced mass transport. Instead, we observe an inverse Blech length phenomenon, which warrants a critical review of the current interconnect design practices.

The observations made in this study are specific to the geometries that allow current-crowding-induced varying temperature field. As mentioned earlier, this setup is the case for the multilevel interconnects in microelectronic devices. For example, device-level interconnects often have bends that are 90° (or lower), as they crisscross other interconnects joining different terminals of transistors etched in a plane. In the process of connections, the interconnects also make junctions, thereby giving rise to current crowding and hence temperature gradient. In addition, with the advent of the 3D architectured microelectronic packages, an effect similar to electromigration-thermomigration coupling may also occur in slightly bigger structures (e.g., with dimensions of approximately 10 μm), such as Cu-filled through silicon via and microbumps of solders. While we discuss the particular case of thin films in this

work, the fundamental findings may be relevant to other components in microelectronic packages also.

V. CONCLUSIONS

Segmented film fabricated in the form of a Blech structure is suitable for studying the effect of sample length on the electromigration-thermomigration-coupling-induced mass transport behavior in Cu film.

In short-duration electromigration tests (e.g., 30, 100, and 180 min), only forward mass transport at the cathode end of the film is discerned at low magnifications. The extent of the forward migration increases with a decrease in the sample length. The forward migration increases linearly with the inverse of the sample length. This result indicates observation of an inverse Blech length phenomenon in these samples.

FEA simulations reveal that both the temperature and the temperature gradient (both the minimum value near the center of the film and the maximum value near the edge of the Cu film) increase upon decreasing the length of the sample. For this reason, the forward-driving force of thermomigration increases and the backward-driving force due to the stress gradient decreases with a decrease in the sample length. This phenomenon can explain the absence of the Blech length effect and observation of the inverse Blech length phenomenon, instead, in a Cu-SiO$_2$/Si system with a W interlayer.

ACKNOWLEDGMENTS

[1] K. N. Tu, Recent advances on electromigration in very-large-scale-integration of interconnects, J. Appl. Phys. **94,** 5451 (2003).

[2] I. A. Blech, Electromigration in thin aluminum films on titanium nitride, J. Appl. Phys. **47,** 1203 (1976).

[3] I. A. Blech, Diffusional back flows during electromigration, Acta Mater. **46,** 3717 (1998).

[4] R. L. de Orio, H. Ceric, and S. Selberherr, Physically based models of electromigration: From Black's equation to modern TCAD models, Microelectron. Rel. **50,** 775 (2010).

[5] I. A. Blech and C. Herring, Stress generation by electromigration, Appl. Phys. Lett. **29,** 131 (1976).

[6] I. A. Blech and K. L. Tai, Measurement of stress gradients generated by electromigration, Appl. Phys. Lett. **30,** 387 (1977).

[7] R. S. Sorbello, Microscopic driving forces for electromigration, Materials Research Society Symposium Proc. **427,** 73 (1996).

[8] E. T. Ogawa, K. D. Lee, V. A. Blaschke, and P. S. Ho, Electromigration reliability issues in dual-damascene Cu interconnections, IEEE Trans. Rel. **51,** 403 (2002).

[9] C. A. Ross, J. S. Drewery, R. E. Somekh, and J. E. Evetts, The effect of anodization on the electromigration drift velocity in aluminum films, J. Appl. Phys. **66,** 2349 (1989).

[10] A. Abbasinasab and M. M. Sadowska, in *Proc. International Symposium on Physical Design (ISPD)* (2015), p. 111.

[11] N. Wang and N. Provatas, Role of Stress-Driven Interfacial Instability in the Failure of Confined Electric Interconnects, Phys. Rev. Appl. **7,** 024032 (2017).

[12] C. J. Meechan and G. W. Lehman, Diffusion of Au and Cu in a temperature gradient, J. Appl. Phys. **33,** 634 (1962).

[13] A. Straub, Ph.D. thesis: Max-Planck-Institute for Metallurgy and Stuttgart University, 2000.

[14] N. Somaiah, D. Sharma, and P. Kumar, Electric current induced forward and anomalous backward mass transport, J. Phys. D: Appl. Phys. **49,** 20LT01 (2016).

[15] N. Somaiah and P. Kumar, Tuning electromigration-thermomigration coupling in Cu/W blech structures, J. App. Phys. **124,** 185102 (2018).

[16] J. T. Trattles, A. G. O'Neill, and B. C. Mecrow, in *Proc. of the VMIC, IEEE* (1991), p. 343.

[17] K. N. Tu, C. C. Yeh, C. Y. Liu, and C. Chen, Effect of current crowding on vacancy diffusion and void formation in electromigration, Appl. Phys. Lett. **76,** 988 (2000).

[18] I. A. Blech and E. Kinsbron, Electromigration in thin gold films on molybdenum surfaces, Thin Solid Films **25,** 327 (1975).

[19] D. Choi, C. S. Kim, D. Naveh, S. Chung, A. P. Warren, N. T. Nuhfer, M. F. Toney, K. R. Coffey, and K. Barmak, Electron mean free path of tungsten and the electrical resistivity of epitaxial (110) tungsten films, Phys. Rev. B **86,** 045432 (2012).

[20] See Supplemental Material at http://link.aps.org/supplemental/10.1103/PhysRevApplied.10.054052 for several figures, such as variation of slope of L$_{cathode}$ versus l^{-1} graph as function of duration of test and FEM simulation results showing variation of electric current density, temperature and temperature density as function of distance from edge of Cu stripes.

[21] G. J. van Gurp, P. J. de Waard, and F. J. du Chatenier, Thermomigration in indium films, Appl. Phys. Lett. **45,** 1054 (1984).

[22] A. T. Huang, A. M. Gusak, K. N. Tu, and Y. S. Lai, Thermomigration in SnPb composite flip chip solder joints, Appl. Phys. Lett. **88,** 141911 (2006).